GEOLOGICA CARPATHICA, APRIL 2010, 61, 2, 111–120 doi: 10.2478/v10096-010-0004-5

Time series analysis (orbital cycles) of the uppermost Cenomanian–Lower Turonian sequence on the southern Tethyan margin using foraminifera

MOHAMED SOUA

Entreprise Tunisienne d'Activités Pétrolières, ETAP-CRDP 4 Rue des Entrepreneurs, 2035 la Charguia II, Tunisia; mohamed.soua@etap.com.tn

(Manuscript received April 30, 2009; accepted in revised form December 11, 2009)

Abstract: Time series analysis has been performed for the first time on the Cenomanian-Turonian sequence in Central Tunisia in order to shed light on its Milankovitch-like cyclicity. This analysis was applied to two foraminiferal genera: the biserial *Heterohelix*, an oxygen-minimum zone (OMZ) dweller, and the triserial *Guembelitria*, a eutrophic surface dweller. Average sedimentary rates and the duration of the oceanic anoxic event (OAE2) in each studied section were estimated. The fluctuations in abundance of these two opportunistic species can be related mainly to both precessional (ca. 20 kyr) and eccentricity (100 and 400 kyr) cyclicity suggesting that changes in surface water fertility were linked to climate changes in the Milankovitch frequency band.

Key words: Cenomanian-Turonian boundary, time series analysis, cyclostratigraphy, Milankovitch cyclicity, *Heterohelix* spp., *Guembelitria* spp.

Introduction

Understanding of the biotic and sedimentary events that marked Earth history is of great interest in the geoscience community (e.g. Haq et al. 1987; Sepkoski 1993; Kauffeman 1995; Sageman et al. 1998; O'Dogherty & Guex 2001; Soua & Tribovillard 2007). The Cenomanian-Turonian (C/T) boundary lies in a time interval characterized by a cluster of significant events, some of which are biotic (mass, step-by-step or even pseudo-extinction (O'Dogherty, personal communication, progressive recolonization of new habitats, etc.), others are sedimentary (forced regression following an intense transgression) (e.g. Robaszynski et al. 1990; Hardenbol et al. 1998; De Wever et al. 2003; Zhao et al. 2004). The chronometric scale across the C/T boundary has been defined by (1) radiometric ages, such as $40^{Ar}/39^{Ar}$ determined from bentonite layers at the Pueblo section (e.g. Obradovich 1993; Kowallis et al. 1995), (2) ammonite biostratigraphy (e.g. Kennedy & Cobban 1991), and (3) linear interpolation (where the sedimentation rate is assumed to be constant) inside the magnetic anomaly C34 (Cretaceous Normal Super-Chron).

It has been suggested that the marl-limestone alternations characterizing the C/T transition in Central Tunisia may have originated from orbital forcing (Vonhof et al. 1998; Nederbragt & Fiorentino 1999; Caron et al. 1999; Soua & Tribovillard 2007). The thus induced climatic changes produced alternations between terrigenous input and pelagic-hemipelagic carbonate sedimentation.

Geological framework

According to the tectonic setting, this area is regarded as being a transitional zone between the Tunisian Northern Atlas, dominated by diapiric salt structures, and the Tunisian Central Atlas, dominated by a NE-SW trending fold axis, which is intersected by many trough faults bordering on Neogene-filled half-graben systems (Soua et al. 2009). The C/T interval is represented by the black shales of the Bahloul Formation (Robaszynski et al. 1990; Maamouri et al. 1994; Caron et al. 1999; Nederbrag & Fiorentino 1999; Soua 2005; Soua et al. 2006, 2009; Soua & Tribovillard 2007) in some localities, the sedimentation was controlled by basin morphology created either by Triassic salt halokinesis (Fig. 1A) affecting the Cretaceous series or by other syn-sedimentary tectonic activities. The eastern part belongs to the Bargou area that is connected paleogeographically to central Tunisia. It is characterized by (1) emerged paleohighs displaying gaps and discontinuities, and by (2) subsiding zones affected by deep-water sedimentation. This area is dominated by N140° and N70° trending faults limiting several blocks.

Uniquely, in the Dir Ouled Yahia (COK) situated in Bargou area and Guern Halfaya (GH) sections, the top of the Bahloul Formation represents many Cenomanian olistolith levels marking syndepositional tectonic activities. Elsewhere, these syn-sedimentary features are represented by local slumping as in the Jerissa (CES) and Hammem Mellegue (HM) sections.

Material and methods

A total of 219 samples were collected throughout the Bahloul Formation, which is well exposed in these four sections (Fig. 1A,B). Calcium carbonate ($CaCO_3$) analysis was conducted in the Geochemistry Laboratory at the Faculty of Science of Tunis University, the total organic carbon (TOC) was determined on crushed samples with a Rock-Eval II type machine in ETAP. Thin section analysis was conducted in the

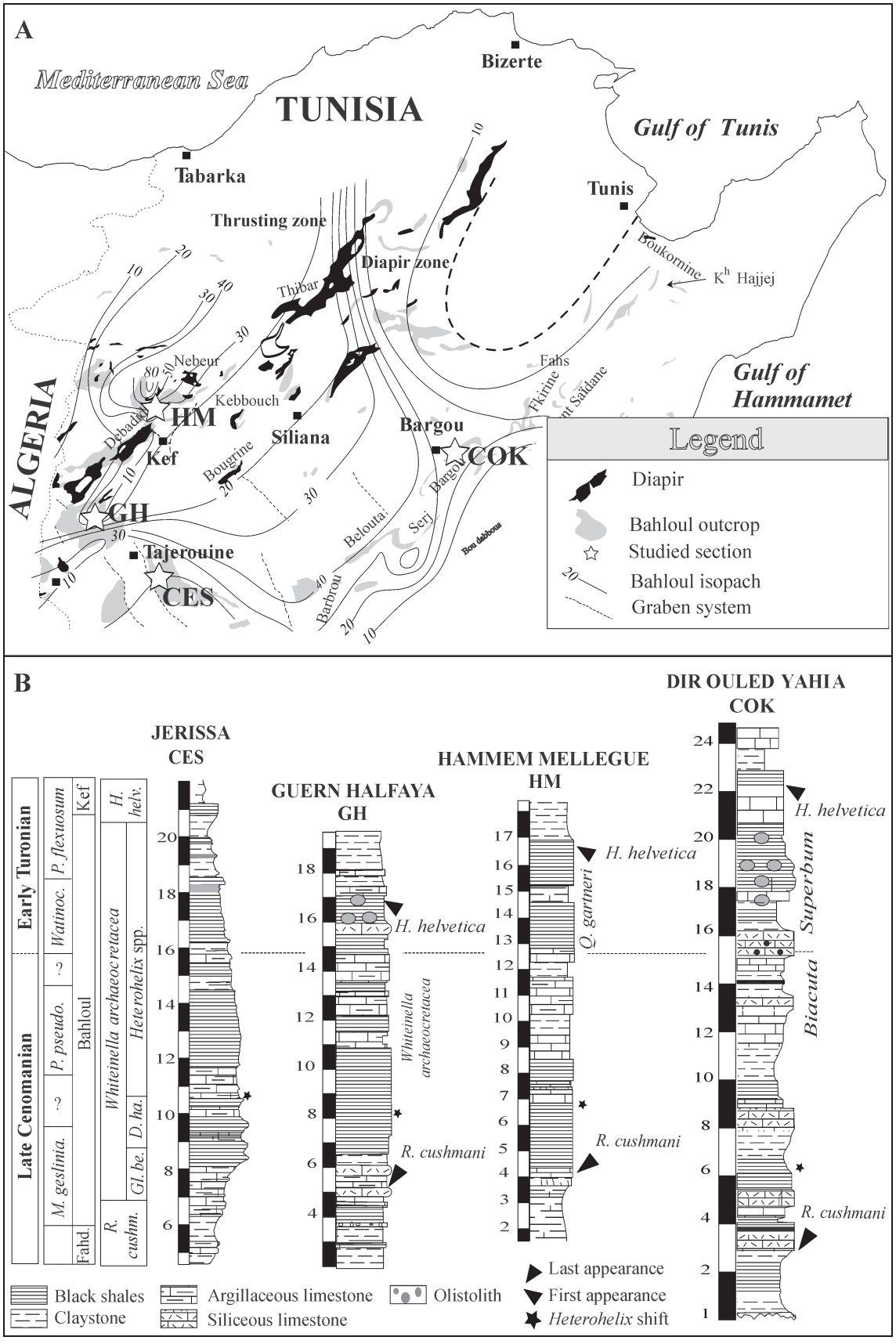

Fig. 1. Location of the studied sections. (**A**) Bahloul isopach map and C/T paleogeography in Central Tunisia. (**B**) Stratigraphy and biostratigraphy of Jerissa (CES), Guern Halfaya (GH), Hammem Mellegue (HM) and Bargou (COK) sections.

geological laboratory of the Office National des Mines (ONM). High-resolution biostratigraphical and geochemical studies have previously been undertaken (Soua 2005; Soua & Tribovillard 2007) and the essential foraminiferal zone and subzone divisions have been established there. In the present paper, only the abundances of *Heterohelix* spp. (total *Heterohelix* species) and *Guembelitria* spp. (total *Guembelitria* species) in each section were used for time series analysis. Spectral analysis was carried out using an integrated software package (PAST, Hammer et al. 2001). Spectral estimation was applied to the *Heterohelix* spp. and *Guembelitria* spp. frequency (%) data series. The use of the spectral estimation ensures a better confidence factor when spectral analysis is used as a cyclostratigraphic tool.

Results

The Bahloul Formation in the studied sections (Fig. 1B) consists of alternating limestone, argillaceous limestone and rhythmically bedded marls. Uniquely, in the Bargou and Guern Halfaya areas (COK and GH sections) it is represented by an original organic-rich and siliceous facies (Soua et al. 2006; Soua & Tribovillard 2007; Fig. 2.3). The Bahloul limestone consists of wackstone/packstone clay-poor carbonates rich in microfossils (filaments, Fig. 2.1; radiolarians, Fig. 2.2; foraminifera, Fig. 2.4; and calcispheres, Fig. 2.5) and macrofossils (ammonites), whereas marls consist of clay-rich carbonates (Robaszynski et al. 1990; Maamouri et al. 1994; Nederbragt & Fiorentino 1999; Caron et al. 1999; Soua 2005;

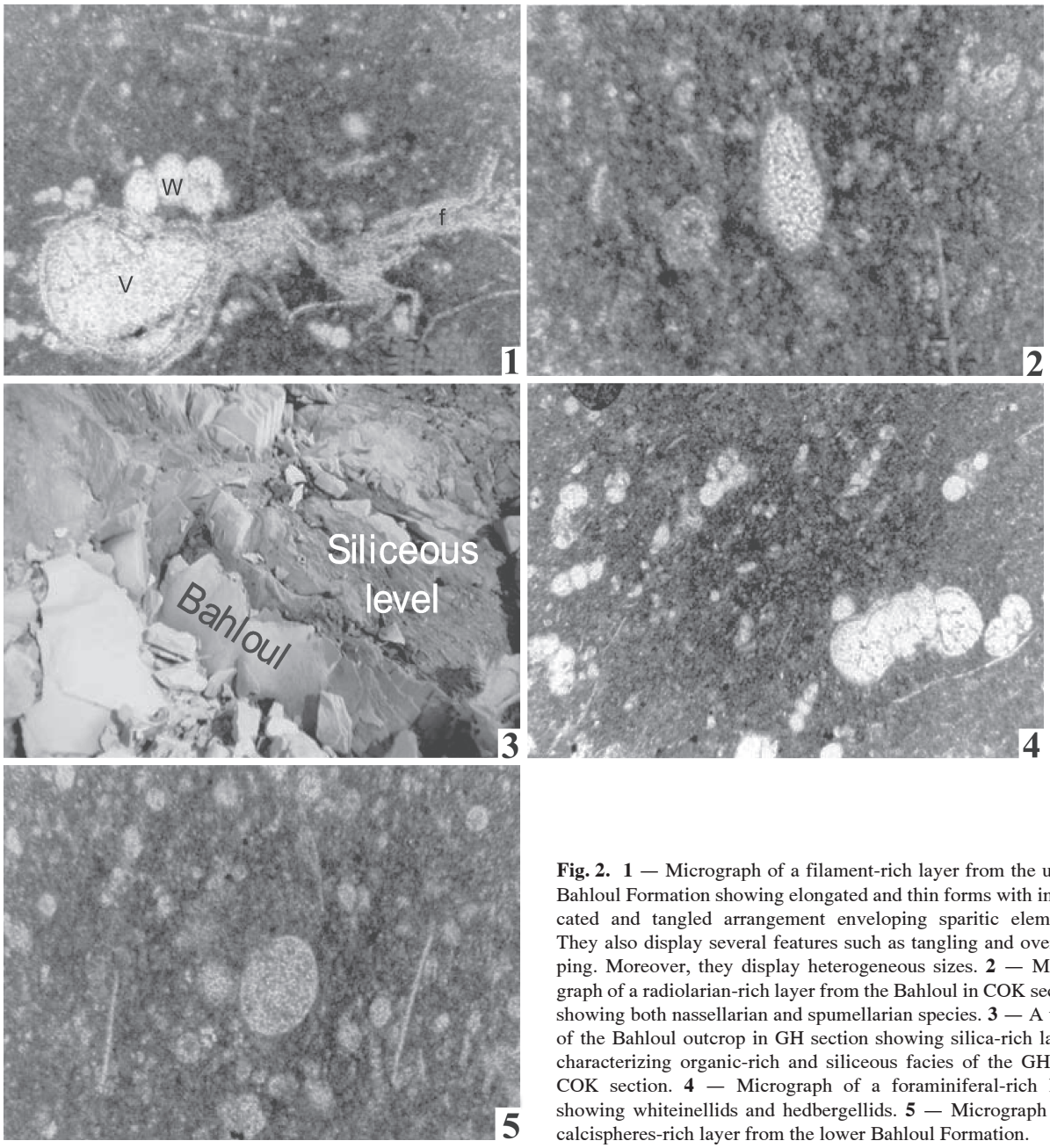

Fig. 2. **1** — Micrograph of a filament-rich layer from the upper Bahloul Formation showing elongated and thin forms with imbricated and tangled arrangement enveloping sparitic elements. They also display several features such as tangling and overlapping. Moreover, they display heterogeneous sizes. **2** — Micrograph of a radiolarian-rich layer from the Bahloul in COK section showing both nassellarian and spumellarian species. **3** — A view of the Bahloul outcrop in GH section showing silica-rich layers characterizing organic-rich and siliceous facies of the GH and COK section. **4** — Micrograph of a foraminiferal-rich level showing whiteinellids and hedbergellids. **5** — Micrograph of a calcispheres-rich layer from the lower Bahloul Formation.

Soua & Tribovillard 2007). According to Caron et al. (1999), periods of low sea levels generally coincide with high detrital influx (marls) and increased erosion and are predominantly associated with arid and/or cooler climatic conditions. Periods of high sea levels are generally characterized by increased carbonate production (limestone) and low detrital influx under warm and humid climatic conditions. The Bahloul black shales are on average about 20 m thick. A prominent microconglomeratic limestone, 50 cm thick on average, marks the base of the Bahloul. It contains a late Cenomanian ammonite assemblage of the *Metoicoceras geslinianum* Zone in the Jerissa (CES) section (Accarie et al. 1999), and a planktonic foraminiferal assemblage indicative of the uppermost *Rotalipora cushmani* Zone. It is composed of grey limestone beds overlain by thinly bedded marls with a few laminated darker limestone beds. These layers are overlain by increasingly clayey limestone beds. In the middle part, the microfauna display a more dissolved aspect and dwarfism. Ammonite-rich and ichnofossil-rich beds are present in the Jerissa (CES), Guern Halfaya (GH) and Bargou (COK) sections (Fig. 1B) and they are used as a correlation tool. Two opportunistic species (the biserial *Heterohelix* and the triserial *Guembelitria* spp.) were selected for this study to carry out spectral analysis. ***Heterohelix*** is considered to be a global biomarker that reflects the expansion of the oxygen-minimum zone (OMZ) (Soua & Tribovillard 2007). This low oxygen tolerant species dominates the faunal assemblages, averaging up to 80 % in the Bahloul black shales (Fig. 3), and especially in the lower *W. archaeocretacea* Zone (Soua & Tribovillard 2007; Fig. 1B; Fig. 3). The ***Guembelitria*** species thrived in eutrophic surface waters with variable salinities at times of severe ecological stress (Soua & Zaghbib-Turki 2007; Soua & Tribovillard 2007).

Time series analysis

In the stratigraphic record, sedimentary rhythmicity has been well discussed and debated (see mainly Berger et al. 1989; House 1995; Weedon 2003). Such records are often interpreted as orbitally controlled especially with the hierarchical stacking of limestone-marl couplets (Berger 1978; House 1995; Negri et al. 2003; Scopelliti et al. 2006). It is believed that periodicities of precession and obliquity were not the same in the past as today (e.g. Berger et al. 1989; Strasser et al. 2006).

Well established correlations between rhythmic sequences and geochemical and biotic parameters have been described by many authors (e.g. Ditchfield & Marshall 1989; Weedon & Jenkyns 1990), confirming temperature dependence and correlations with % $CaCO_3$, nannofossils and foraminifera frequencies (%), which might be expected to be controlled by temperature or other parameters related to Milankovitch cyclicity (House 1995; Negri et al. 2003). The frequency distribution of limestone-marl alternations and their relation to the Milankovitch parameters is commonly tested by time series analysis (e.g. House 1986, 1995; Weedon 2003). The power spectrum shows generally squared amplitudes and wavelengths that represent the periods of regular components in the time series (Weedon 2003). Conventionally, the horizontal axis of the power spectrum represents *Frequency* (Frequency = 1/period) with the highest frequencies (i.e. shortest oscillations) appearing on the right and the vertical axis represents *Power spectra* (Fig. 3). Zero frequency usually corresponds to oscillations that have periods exceeding the length of the whole data set (Weedon 2003). The *Heterohelix* spp. and *Guembelitria* spp. relative abundance curves in the four localities clearly exhibit strong cyclic signals (Fig. 3), which allowed us to perform a spectral analysis study, computed using the PAST software (Hammer et al. 2001), to test for the existence of periodicities through the oceanic anoxic event (OAE2) deposits in Central Tunisia. The results of the spectral analysis are illustrated in Fig. 3. The strongest peaks point to a period of 25 m (*Heterohelix* spp.) in the HM section (Fig. 3A) and a period of 17.54 m (*Guembelitria* spp.) in the CES section (Fig. 3D).

Hammem Mellegue (HM section)

Nederbragt & Fiorentino (1999) argued that in the nearby Mellegue section the Bahloul Formation is suggestive of Milankovitch cycles due to its regular strata (Fig. 1B). Average accumulation rates of about 10 cm/kyr for the same Bahloul interval was previously determined by Vonhof et al. (1998) suggesting that each 2-m-thick pair of laminated limestone and bioturbated marly limestone represents a precession cycle (20 kyr) rather than an obliquity cycle (40 kyr) as seen in other C/T intervals (e.g. Arthur et al. 1987; Kuhnt et al. 1997; Sageman et al. 1998). Time series analysis performed on *Heterohelix* spp. shows that the strongest peak points to a period of 25 m (Fig. 3A). Other statistically significant peaks are found at 11.9 m and 5.26 m. This latter peak, although statistically significant, falls in the low-energy field of the spectrum. The spectral curve of the *Guembelitria* spp. shows significant peaks at about 15.62 m and 7.14 m. The 4.54 m and 3.12 m peaks (Fig. 3A) recorded in the low energy field of the spectrum are very close, and they might be considered as components of the same periodicity.

Dir Ouled Yahia (COK section, Bargou area) and Guern Halfaya (GH section)

The COK section, about 24 m thick (Fig. 1B), is exposed in Oued El Kharroub (Bargou area) (Fig. 1A), whereas the GH section, about 17 m thick, is located between Hammem Mellegue and Tajerouine and is one of the most expanded CT transitions in Tunisia (Soua & Tribovillard 2007). The results of the spectral analysis are also shown in Fig. 3 (B and C). At the COK and GH sections, the Bahloul Formation is characterized by several radiolarian-rich siliceous beds (Soua et al. 2006; Fig. 2.3). The time series analysis performed on *Heterohelix* spp. shows that the strongest peak points to a period of 17.85 m (Fig. 3B). Other significant values are represented at 9.1 m, 5 m and 3.84 m.

Dealing with *Guembelitria* time series analysis, we observe strong peaks at 13.16 m and 12.82 m respectively in the GH and COK sections (Fig. 3B; Fig. 3C).

Jerissa (CES section)

The *Heterohelix* signal was filtered and three significant peaks of different wavelengths were detected (i.e. 19.6 m,

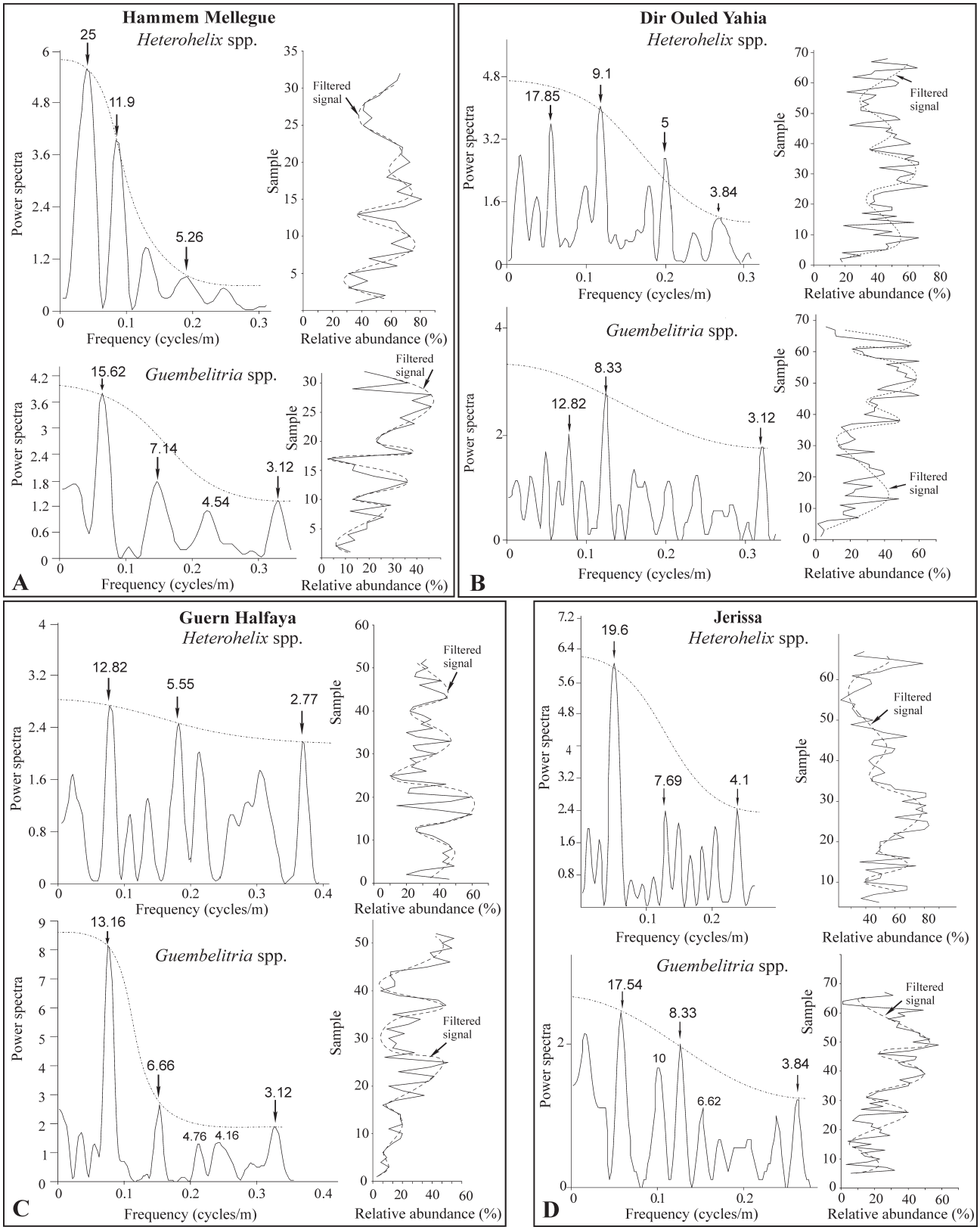

Fig. 3. A–D — Time series analyses performed on the two opportunistic C/T foraminiferal species, the OMZ dweller *Heterohelix* spp. and the eutrophic surface dweller *Guembelitria* spp. showing the power spectrum of their relative abundance logs (%) in the studied interval of the Bahloul in each section. The values on the vertical axis indicate the power while the horizontal axis refers to frequencies in cycles/meter, from low-frequency (left) to high-frequency (right) periodicities. Only the statistically significant periodicities are labelled; numbers above the significant peaks are frequencies in cycle meter. Dashed lines indicate filtered signals.

7.69 m, and 4.1 m; Fig. 3D). They were selected for this study because they represent accurate values for time series analysis. These values are normalized to the shortest periodicity (i.e. 4.1) and then compared to the relative precession ratios of classical Milankovitch periodicities (see Table 1). Table 1 shows the relationship between the ratios obtained by the normalization both of the eccentricity (100–400 kyr) and obliquity (40 kyr) to the precession (20 kyr). All wavelengths (related respectively to *Heterohelix* and *Guembelitria* in the four sections) are normalized to the related shortest periodicity.

Cyclostratigraphy

According to the Park & Oglesby (1991) model, which reproduces Cretaceous Milankovitch cyclicity, the Bahloul sequence may display a Milankovitch style climatic cyclicity corresponding to a 20 kyr precession cycle that prevailed at low latitudes during the C/T transition. In this study we have tried to calculate the paleolatitudes of the Kef and Bargou areas (where the four studied sections are situated) during the C/T transition, namely about 93.5 Ma. The calculated paleolatitudes are about 15 to 17° N according to Philip et al. (1993), or 16–19° N according to Camoin et al. (1993). In contrast they are 37° to 37.5° N according to the ODSN Plate Tectonic Reconstruction Service (Hay et al. 1999).

These latter sequences represent variable indurate levels that also show % TOC, % $CaCO_3$ and ‰ $\delta^{13}C$ fluctuations (Fig. 5).

Influence of orbital forcing during Bahloul deposition

Negri et al. (2003) discussed the duration of the orbital cycles in a time-equivalent Bonarelli black shale level, and have shown that they can be normalized and tuned to precession cycles. The *Heterohelix* and *Guembelitria* signals in the studied sections were filtered, and show significant fluctuations in the OMZ and eutrophic surface dweller signals (see Fig. 4).

This time series analysis allowed us to develop a cyclostratigraphic approach in order to estimate the duration of the organic-rich Bahloul Formation in the four studied sections. The evaluation of the OAE2 duration was the subject of several studies and was originally estimated based mainly on biostratigraphic (ammonites and foraminiferal) ranges (e.g. Hardenbol et al. 1998) and/or orbital cyclicity. Estimates are: 720 kyr in the Pueblo section (Meyers et al. 2004), about 400 kyr in Tarfaya and Wadi Bahloul (Kuhnt et al. 1997; Caron et al. 1999), 320 kyr in western Canada and the Bottaccione section in Central Italy (Prokoph et al. 2001; Scopelliti et al. 2006), 450 kyr for the Douvres section (Gale 1991), 500 kyr to 600 kyr for the Thomel level (Morel 1998). Wavelength ratios were tuned to the associated orbital cyclicity of the C/T transition strata (see Table 1). Alternatively we may estimate an average sedimentary rate for the Bahloul Formation (OAE2) by tuning each calculated wavelength to the corresponding orbital cyclicity (e.g. 19.6/100; 7.69/40; 4.1/20; *Heterohelix* data of the CES section). Figure 4 shows that for the CES section, the *Heterohelix* precession curve (filter 20) exhibits 18 to 19 cycles. This means that a duration of about 400 kyr can be attributed to the Bahloul Formation, which represents the anoxic event. The eccentricity curve exhibits about 4 to 4.5 cycles, which also corresponds to about (i.e. ~400 kyr). The average duration of the Bahloul Formation (OAE2) may thus be evaluated as ~400 kyr. The results are displayed in Fig. 4, and Table 1.

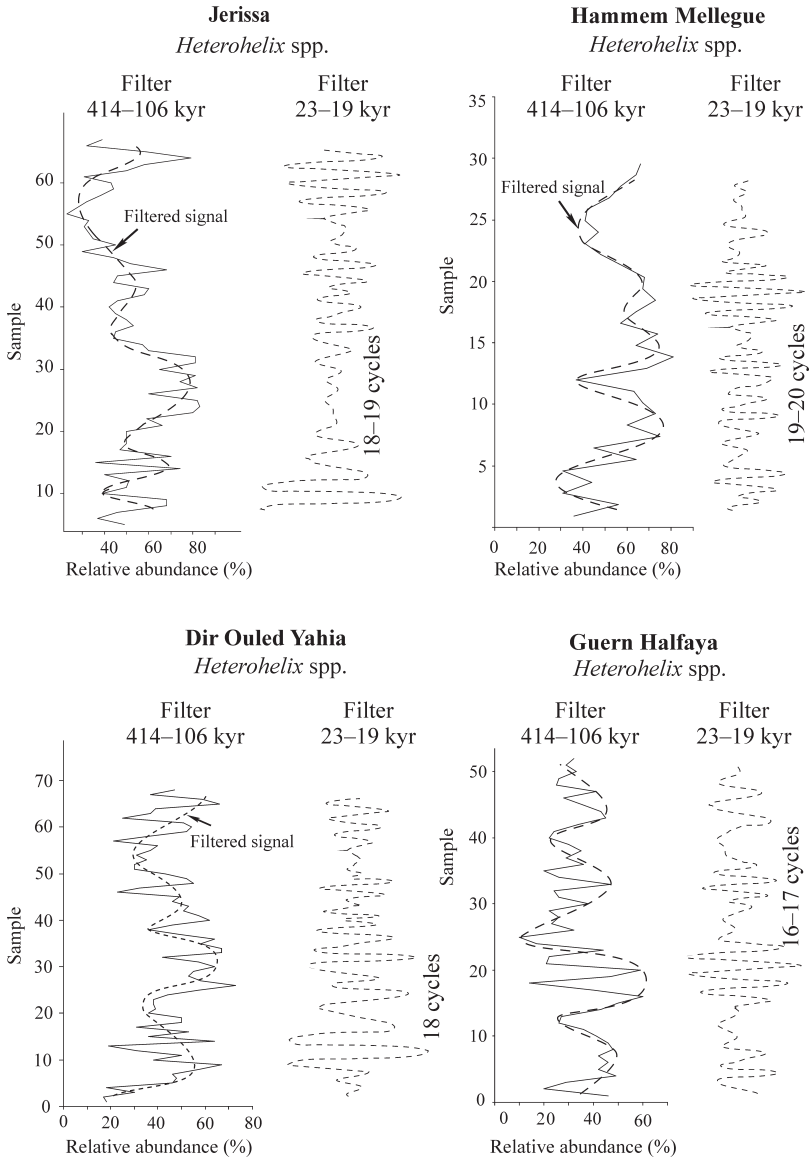

Fig. 4. Comparison between the filtered signals (precession and eccentricity) of the *Heterohelix* spp. of the four studied sections.

Table 1: Wavelengths evaluated from the power spectra in Fig. 3; average sedimentary rates (cm/kyr) and estimated duration of the OAE2 in each section. Note that the Bahloul Formation is deposited within an interval of 350–410 kyr with a sedimentation rate encompassed between 12 and 20 cm/kyr.

Section	Orbital perturbation	Duration at present time (kyr)	Average ratios relative to Precession	Wavelengths (*Heterohelix*)	Wavelengths (*Guembelitria*)	Wavelength ratios (*Heterohelix*)	Wavelength ratios (*Guebelitria*)	Average sedimentation rate (cm/kyr)	OAE2 duration
COK	**Eccentricity**	100 400	12.8 4.6	17.85	12.82	4.6	4.1	14	~380 kyr
	Obliquity	40	2.8 1.8	9.1	8.33	2.4	2.6	18	
	Precession	20	1	3.84	3.12	1	1	16	
GH	**Eccentricity**	100 400	12.8 4.6	12.82	13.16	4.6	4.2	11	~350 kyr
	Obliquity	40	2.8 1.8	5.55	6.66	2	2.1	12	
	Precession	20	1	2.77	3.12	1	1	13	
HM	**Eccentricity**	100 400	12.8 4.6	25	15.62	4.8	5	18	~410 kyr
	Obliquity	40	2.8 1.8	11.9	7.14	2.26	2.28	20	
	Precession	20	1	5.26	3.12	1	1	20	
CES	**Eccentricity**	100 400	12.8 4.6	19.6	17.54	4.7	4.5	17	~400 kyr
	Obliquity	40	2.8 1.8	7.69	8.33	1.9	2.1	16	
	Precession	20	1	4.1	3.84	1	1	18	

Discussion

The solar influx which penetrates the atmosphere is controlled by the orbital parameters of the Earth: namely eccentricity, obliquity and precession (Berger 1978; House 1995). These orbital variations lead to climatic variations, which then influence oceanic circulation and the sedimentary systems. A dominance of precession cycles on climate change and sedimentation can be discerned during the C/T interval (Berger 1978). In addition, ignoring the obliquity signal component will greatly simplify data interpretation (Vonhof et al. 1998; Nederbragt & Fiorentino 1999; Caron et al. 1999; Negri et al. 2003; Scopelliti et al. 2004). Eccentricity is known to be very stable through the Mesozoic time and did not vary significantly through the last 100 Ma (Laskar 1989, 1999; Berger et al. 1992). Figure 3 and Figure 4 show the cyclostratigraphic interpretation of the four studied sections, leading to the recognition of precession cycles and the identification of 100 kyr cycles (short eccentricity). The spectral analysis applied to the *Heterohelix/Guembelitria* spp. fluctuations (Fig. 3) points to the presence of a meter-scale periodicity, for example at 25 m in the HM section (Fig. 3A), and other major relevant peaks at 11.9 m and 5.26 m using *Heterohelix* spp. counts. Regarding *Guembelitria* ssp., there is a meter-scale periodicity at 17.54 m in the CES section and other important peaks at 8.33 and 3.84 m (Fig. 3D). The relationship between the ratios obtained by the normalization both of the eccentricity (100–400 kyr) and obliquity (40 kyr) to the precession (20 kyr) are displayed in Table 1. The high correlation between the spectral peak ratios (of both the *Heterohelix* and *Guembelitria* in the four sections) and those of the orbital components is very interesting (Fig. 3A, Table 1). Calculated average sedimentary rates (Table 1) are in perfect agreement with the sedimentation rate estimated from Hardenbol et al. (1998) and the relatively close value (10 cm/kyr) obtained by Vanhof et al. (1998) for the Mellegue section. This interpretation clearly highlights the existence of cyclicity within the Bahloul Formation that is more complex than that which can be recognized by visual inspection. It implies that orbital forcing has caused the *Heterohelix* and *Guembelitria* abundance fluctuations.

Paleoecology of the two opportunistic species

The biserial heterohelicids (*Heterohelix* spp.), are believed to be ecological opportunists and low-oxygen tolerant fauna, which thrive in well-stratified open marine settings with a well-developed oxygen minimum zone (OMZ) (Boersma & Premoli Silva 1988; Barrera & Keller 1994). Thus, high abundance of *Heterohelix* indicates an expanded oxygen minimum zone (Soua & Tribovillard 2007).

The triserial heterohelicacea *Guembelitria* species thrived in eutrophic surface waters with variable salinities at times of severe ecological stress (Leckie 1987; Kroon & Nederbragt 1990; Soua & Tribovillard 2007; Soua & Zaghbib-Turki 2007).

Relationship between paleoecology and the orbital cycles

We have shown that in the four studied sections strong cyclicity is reflected not only in the lithological pattern but also

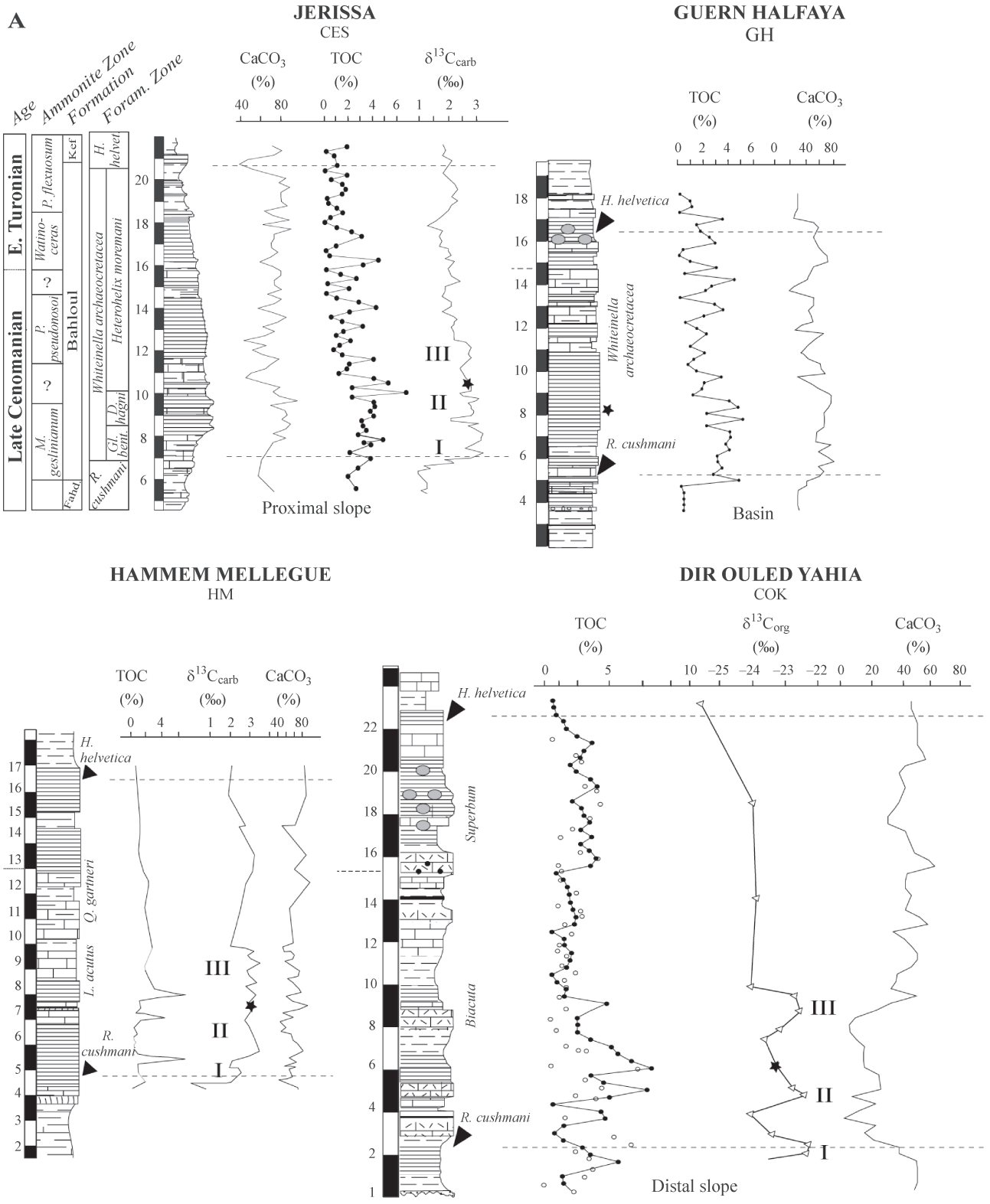

Fig. 5A — Geochemical (% $CaCO_3$; % TOC and % $\delta^{13}C$) and biostratigraphic (foraminifera, radiolarians and ammonites) data of the four studied sections (modified from Soua & Tribovillard 2007). I, II and III indicate the three worldwide isotopic spikes of the C/T boundary. Black stars indicate the *Heterohelix* shift (within each section).

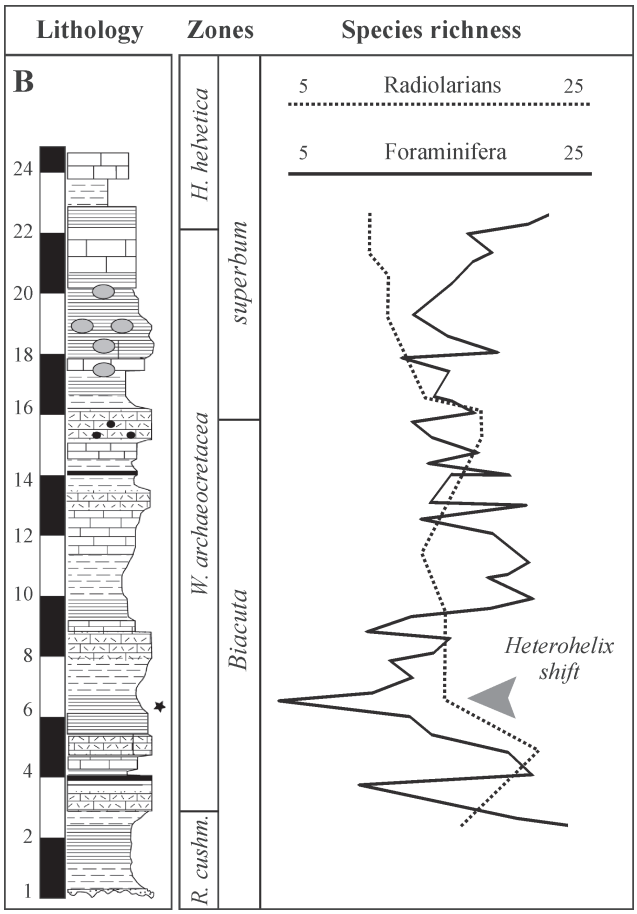

Fig. 5B — Distribution and correlation of foraminiferal and radiolarians profiles in the same graphic at Bargou section.

in the biotic signal. In particular, our data recognize a strong precessional signal that is comparable to others identified all over the world (Kuhnt et al. 1997; Morel 1998; Caron et al. 1999; Prokoph et al. 2001; Negri et al. 2003; Meyers et al. 2004; Scopelliti et al. 2006). The paleoecological preferences of both *Heterohelix* spp. and *Guembelitria* spp. seem to be related to areas of enhanced surface water fertility and oxygene-minimum zone (e.g. Nederbragt & Fierontino 1999; Luning et al. 2004; Soua & Tribovillard 2007). Thus, the long term fluctuations related to both precession and eccentricity suggest that changes in surface water fertility were linked to the Milankovitch parameters.

Conclusion

Four C/T transition sections were sampled in Central Tunisia displaying biotic and lithological variations. Time series analysis was applied to the abundances of two opportunistic foraminiferal genera (*Heterohelix* and *Guembelitria* spp.) for all the four sections. This analysis allowed us to calculate and estimate both the average sedimentary rate and the duration of the OAE2 in each section. In addition, the biotic signal represented by the *Heterohelix* and *Guembelitria* spp. relative abundance fluctuations in the studied sections is probably driven by Milankovitch frequencies through a climate-controlled productivity model. We can deduce that the fluctuations of these two species are related mainly to both precessional and eccentricity cyclicity, suggesting that changes in surface water fertility were linked to the Milankovitch parameters. Thus the Bahloul Formation in the four studied sections exhibits a duration interval between 350–400 kyr and a sedimentation rate interval between 12 and 20 cm/kyr.

Acknowledgment: Prof. André Strasser provided a thorough review of this article and has made numerous suggestions to improve the text. The author is also grateful to the reviewers, Dr. Jozef Michalík (Responsible Editor) and Prof. Adam Gasiński (Jagiellonian University) for providing constructive comments and Nigel Collins (Terrasciences Ltd.) for improving the English.

References

Accarie M., Robaszynski F., Amedro F., Caron M. & Zagrarni M.F. 1999: Stratigraphie événementielle au passage Cénomanien–Turonien dans le secteur occidental de la plateforme de Tunisie centrale (Formation Bahloul, région Kalaat Senen). *Ann. Min. Géol.* 40, 63–80.

Arthur M.A., Schlanger S.O. & Jenkyns H.C. 1987: The Cenomanian–Turonian oceanic anoxia event: II. Paleoceanographic controls on organic matter production and preservation. In: Brooks J. & Fleet A.J. (Eds.): Marine and petroleum source rocks. *Geol. Soc. London, Spec. Publ.* 26, 401–420.

Barrera E. & Keller G. 1994: Productivity across the Cretaceous-Tertiary boundary in high latitudes. *Geol. Soc. Amer. Bull.* 106, 1254–1266.

Berger A.L. 1976: Obliquity and precession for the last 5,000,000 years. *Astromony and Astrophysics* 51, 127–135.

Berger A.L. 1978: Long-term variations of caloric insolation resulting from the Earth's orbital elements. *Quat. Res.* 9, 139–167.

Boersma A. & Premoli Silva I. 1988: Atlantic Palaeogene biserial heterohelicid foraminifers and oxygen minima. *Palaeoceanography* 4, 271–286.

Camoin G., Bellion Y., Dercourt J., Guiraud R., Lucas J., Poisson A., Ricou L.E. & Vrielynck B. 1993: Late Maastrichtian (69.5–65 Ma). In: Dercourt J., Ricou L.E. & Vrielinck B. (Eds.): Atlas Tethys palaeoenvironmental maps. Explanatory notes. *Gauthier-Villars*, Paris, 179–196.

Caron M., Robaszynski F., Amedro F., Baudin F., Deckonink J.F., Hochuli P., Salis Perch Nielsen K. (von) & Tribovillard N. 1999: Estimation de la durée de l'événement anoxique global au passage Cénomanien Turonien. Approche cyclostratigraphique dans la Formation Bahloul en Tunisie centrale. *Bull. Soc. Géol. France,* 170, 2, 145–160.

Ditchfield P. & Marshall J.O. 1989: Isotopic variation in rhythmically bedded chalks: paleotemperature variation in the Upper Cretaceous. *Geology* 17, 842–845.

Fischer A.G., Herbert T.D., Napoleone G., Premoli Silva I. & Ripepe M. 1991: Albian pelagic rhythms (Piobbico Core). *J. Sed. Petrology* 61, 1164–1172.

Gale A.S., Jenkyns H.C., Kennedy W.J. & Corfield R.M. 1993: Chemostratigraphy versus biostratigraphy: data from around the Cenomanian Turonian boundary. *J. Geol. Soc. London* 150, 1993, 29–32.

Hammer Ø., Harper D.A.T. & Ryan P.D. 2001: PAST: Paleontological Statistics software package for education and data analysis. *Palaeontologia Electronica* 4, 1, 4, 1–9.

Haq B.U., Hardenbol J. & Vail P.R. 1987: Chronology of fluctuating sea levels since the Triassic. *Science* 235, 1156–1167.

Hardenbol J., Thierry J., Farley M.B., Jacquin T., De Graciansky P.-C. & Vail P.-R. 1998: Cretaceous sequence chronostratigraphy. In: De Graciansky P.-C., Hardenbol J., Jacquin T. & Vail P.R. (Eds.): Mesozoic and Cenozoic sequence stratigraphy of European Basins. *Soc. Econ. Paleontol. Mineral. Spec. Publ.,* Vol. 60, Chart 4.

Hay W., DeConto R., Wold C.N., Wilson K.M., Voigt S., Schulz M., Wold-Rossby A., Dullo W.-C., Ronov A.B., Balukhovsky A.N. & Soeding E. 1999: Alternative global Cretaceous paleogeography. In: Barrera E. & Johnson C. (Eds.): The evolution of Cretaceous ocean/climate systems. *Geol. Soc. Amer., Spec. Pap.* 332, 1–47.

Hinnov L.A. & Goldhammer R.K. 1991: Spectral analysis of the Middle Triassic Latemar Limestone. *J. Sed. Petrology* 61, 1173–1193.

House M.R. 1995: Orbital forcing timescales: an introduction. *Geol. Soc. London, Spec. Publ.* 1995, 85, 1–18.

Kauffman E.G. 1995: Global change leading to biodiversity crisis in a Greenhouse World: The Cenomanian–Turonian (Cretaceous) mass extinction — effects of past global change on life. *National Academy Press*, 48–71.

Kroon D. & Nederbragt A.J. 1990: Ecology and palaeoecology of triserial planktic foraminifers. *Mar. Micropaleontology* 16, 25–38.

Kuhnt W., Nederbragt A. & Leine L. 1997: Cyclicity of Cenomanian–Turonian organic-carbon-rich sediments in the Tarfaya Atlantic coastal basin (Morocco). *Cretaceous Research* 18, 587–601.

Laskar J. 1989: A numerical experiment on the chaotic behaviour of the solar system. *Nature* 338, 237–238.

Leckie R.M. 1987: Paleoecology of mid-Cretaceous planktic foraminifera: a comparison of open ocean and epicontinental sea assemblages. *Micropaleontology* 33, 164–176.

Luning S., Kolonic S., Belhaj E.M., Belhaj Z., Cota L., Baric G. & Wagner T. 2004: An integrated depositional model for the Cenomanian-Turonian organic-rich strata in North Africa. *Earth Sci. Rev.* 64, 1–2, 51–117.

Maâmouri A.L., Zaghbib-Turki D., Matmati M.F., Chikhaoui M. & Salaj J. 1994: La formation Bahloul en Tunisie centro-septentrionale: variation latérales nouvelle datation et nouvelle interprétation en terme de stratigraphie séquentielle. *J. African Earth Sci.* 18, 1, 37–50, 1994.

Morel L. 1998: Stratigraphie à haute résolution du passage Cénomanien–Turonien. *Thèse de l'Université Pierre et Marie Curie*, Paris, VI, 1–224 (Unpublished).

Nederbragt A.J. & Fiorentino A. 1999: Stratigraphy and paleoceanography of the Cenomanian-Turonian Boundary Event in Oued Mellegue, north-western Tunisia. *Cretaceous Research* 20, 47–62.

Negri A., Cobianchi M., Luciani V., Fraboni R. & Milani A.M. Claps 2003: Tethyan Cenomanian pelagic rhythmic sedimentation and Pleistocene Mediterranean sapropels: is the biotic signal comparable? *Palaeogeogr. Palaeoclimatol. Palaeoecol.* 190, 373–397.

O'Dogherty L. & Guex J. 2001: Rates and pattern of evolution among Cretaceous radiolarians: Relations with Global Paleoceanographic Events. *Micropaleontology* Vol. 48, Supplement 1: Micropaleontology of radiolarians: Proceedings of INTERRAD 9 (2001), 1–22.

Park J. & Oglesby R.J. 1991: Milankovitch rhythms in the Cretaceous: a GCM modelling study. *Glob. Planet. Change* 1991, 4, 4, 329–355 (2 p.)

Paul C.R.C., Lamolda M.A., Mitchel S.F., Vaziri M.R., Gorostidi A. & Marshall J.D. 1999: The Cenomanian-Turonian boundary at Eastbourne (Sussex, UK): a proposed European reference section. *Palaeogeogr. Palaeoclimatol. Palaeoecol.* 150, 83–121.

Philip J. et al. 1993 : Late Cenomanian (94–92 Ma). In: Dercourt J. et al. (Eds.): Atlas Tethys, palaeoenvironmental maps. Explanatory notes. *Gauthier-Villars*, Paris, 153–178.

Prokoph A., Villeneuve M., Agterberg F.P. & Rachold V. 2001: Geochronology and calibration of global Milankovitch cyclicity at the Cenomanian-Turonian boundary. *Geology* 29, 523–526.

Robaszynski F., Caron M., Dupuis C., Amedro F., Gonzalez-Donso J.M., Linares D., Hardenbol J., Gartner J., Calandra F. & Deloffre R. 1990: A tentative integrated stratigraphy in the Turonian of Central Tunisia: Formations, zones and sequential stratigraphy in the Kalaat Senan area. *Bull. Centres Rech. Explor. Prod. Elf-Aquitaine* 14, 1, 213–384.

Sageman B., Rich J., Savrda C.E., Bralower T., Arthur M.A. & Dean W.E. 1998: Multiple Milankovitch cycles in the Bridge Creek Limestone (Cenomanian–Turonian), Western Interior basin. In: Arthur M.A. & Dean W.E. (Eds.): Stratigraphy and paleoenvironments of the Cretaceous Western Interior seaway, USA. *Soc. Sed. Geol., Concepts in Sedimentology and Paleontology* 6, 153–171.

Scopelliti G., Bellanca A., Coccioni R., Luciani V., Neri R., Baudin F., Chiari M. & Marcucci M. 2004: High-resolution geochemical and biotic records of the Tethyan 'Bonarelli Level' (OAE2, latest Cenomanian) from the Calabianca–Guidaloca composite section, northwestern Sicily, Italy. *Palaeogeogr. Palaeoclimatol. Palaeoecol.* 208, 293–317.

Sepkoski J., Jr. 1993: Ten years in the library: New data confirm paleontological patterns. *Paleobiology* 19, 43–51.

Soua M. 2005: Biostratigraphie de haute résolution des foraminifères planctoniques du passage Cénomanien Turonien et impact de l'événement anoxique EAO-2 sur ce groupe dans la marge sud de la Téthys, exemple régions de Jerissa et Bargou. *Mém. Mastère, Univ. Tunis, El Manar*, 1–169.

Soua M. & Tribovillard N. 2007: Depositional model at the Cenomanian/Turonian boundary for the Bahloul Formation, Tunisia. *Comptes rendus – Geoscience* 339, 10, 692–701.

Soua M. & Zaghbib-Turki D. 2007: Biotic response during times of severe ecological stress, how paleoceanographic changes in latest Cenomanian–earliest Turonian Ocean induced step-by-step extinction and dwarfism. *Geol. Soc. Amer., Northeastern Section — 42nd Annual Meeting (12–14 March 2007), Paper No. 29–4, Session No. 29.*

Soua M., Zaghbib-Turki D. & O'Dogherty L. 2006: Radiolarian biotic responses to the Latest Cenomanian global event across the southern Tethyan margin (Tunisia). *Proceeding of the tenth Exploration and Production Conference. Memoir* 26, 195–216.

Soua M., Echihi O., Herkat M., Zaghbib-Turki D., Smaoui J., Fakhfakh-Ben Jemia H. & Belghaji H. 2009: Structural context of the paleogeography of the Cenomanian-Turonian anoxic event in the eastern Atlas basins of the Maghreb. *Comptes rendus Geosci.* 341, 12, 1029–1037.

Tsikos H., Jenkyns H.C., Walsworth-Bell B., Petrizzo M.R., Forster A., Kolonic S., Erba E., Premoli Silva I., Baas M., Wagner T. & Sinninghe Damsté J.S. 2004a: Carbon-isotope stratigraphy recorded by the Cenomanian–Turonian oceanic anoxic event: correlation and implications based on three keylocalities. *J. Geol. Soc. London* 161, 711–720.

Vonhof H.B., Nederbragt A.J., Kuypers M., Van Hinte J.E., Ganssen G.M. & Smit J. 1998: Synchronous strontium and carbon isotope excursions across the Cenomanian-Turonian Oceanic Anoxic Event. In: Vonhof H.B. (Ed.): The strontium isotope stratigraphic record of selected geologic events. *PhD Thesis,* Free University, Amsterdam, 93–109.

Weedon G.P. 2003: Time-series analysis and cyclostratigraphy. *Cambridge University Press*, 1–274.

Weedon G.P. & Jenkyns H.C. 1990: Regular and irregular climatic cycles and the Belemnite Marls (Pliensbachian, Lower Jurassic, Wessex Basin). *J. Geol. Soc. London* 147, 915–918.

Zhao X., Riisager P., Riisager J., Draeger U., Coe R.S. & Zheng Z. 2004: New palaeointensity results from Cretaceous basalt of Inner Mongolia, China. *Phys. Earth Planet. Int.* 141, 2, 16, 131–140.